ISSN 1070-3632, Russian Journal of General Chemistry, 2009, Vol. 79, No. 6, pp. 1400–1411. © Pleiades Publishing, Ltd., 2009.
Original Russian Text © V.A. Matyshak, V.F. Tret'yakov, 2009, published in Rossiiskii Khimicheskii Zhurnal, 2009, Vol. 52, No. 4, pp. 151–160.

Role of Surface Structures on the Selective Reduction of Nitrogen Oxides with Hydrocarbons on Oxide Catalysts

V. A. Matyshak[a] **and V. F. Tret'yakov**[b]

[a] *Semenov Institute of Chemical Physics, Russian Academy of Sciences, Moscow, Russia*
[b] *Topchiev Institute of Petrochemical Synthesis, Russian Academy of Sciences (IPS RAS),*
Leninskii pr. 29, Moscow, 119991 Russia
e-mail tretjakov@ips.ac.ru

Received March 3, 2008

Abstract—The infrared spectrum in situ was used to study the mechanism of selective reduction of nitrogen oxides on a series of oxide catalysts. It is shown that under the reaction conditions, nitrites, nitrates, and nitro-organic and acetate complexes are formed. Qualitative comparison of the rate of decomposition of the complexes and the rate of formation of the process products was performed using the spectral kinetic technique. Based on this comparison, the role of surface complexes in the process was determined. A mechanism showing the main stages of the reduction of nitrogen oxides is proposed.

DOI: 10.1134/S1070363209060541

In view of the demand for purification of diesel exhaust gases over the past years much attention has been paid to development of catalysts for selective reduction of nitrogen oxides with hydrocarbons under excess oxygen (NO_x SCR). Sufficiently high activity of copper-containing zeolites in this reaction [1, 2] and principal possibility of selective reduction of nitrogen oxides in the presence of oxygen have been demonstrated. Mechanistic research on this process [3–7] showed that the catalytic activity is associated with isolated copper centers on which molecular adsorption of oxygen is weak and dissociative adsorption is almost lacking. As a result, nitrogen oxides and oxygen do not compete for sites on the surface.

The NO_x SCR process can also be performed on oxide systems [8–11]. In this case, oxygen favors rather than prevents activation of nitrogen oxide as surface nitrate complexes [12–20] which react with hydrocarbons or their activation products to form nitrogen-containing compounds, primarily organic nitrites $ONO–C_mH_n$ or nitrates $O_2N–C_mH_n$ [23–36].

The results of research on the activation of hydrocarbons on their interaction with catalyst surface have been summarized by Captain and Amiridis [37]. The activation of hydrocarbons, in particular propylene, on Broensted centers of catalyst, involves initial formation of an isopropoxide complex, after which acetone and acetate form one after another. Activation on Lewis centers forms acrolein or acrylic acid and then acrylate and acetate. Any of the mentioned forms can take part in forming nitrogen-containing organic compounds and reduction of nitrogen oxides [18, 19, 21, 22].

At elevated temperatures nitrogen-containing organic compounds react with $(NO + O_2)/NO_2$ to form molecular nitrogen or OCN^- [34, 36], NC^- [36, 37], ammonia [26, 29, 32], organic nitriles [29], cyan [39], and hydrocyanic acid [39, 40]. Surface isocyanates which are the most stable and frequently registered decomposition products readily reduce nitrogen oxides to molecular nitrogen and N_2O [34, 36, 38, 40–42]. One more route may involve the reaction of isocyanate with water to form ammonia which, in the presence of NO_x, converts into ammonium nitrite [23–26]. The latter decomposes into molecular nitrogen in the gas phase.

By now certain, fairly common properties of surface nitrite–nitrate and nitro-organic compounds have been established, but the information on the stages of formation of these complexes, structure of the organic part of the nitro compounds, mechanism of transformation of the nitrate complex into molecular nitrogen, and the role of oxygen and nitrogen oxides in this process is completely lacking. Of particular importance, in terms of controlling the activity and selectivity of the NO_x SCR process, is the information concerning the role of the nature of catalyst in surface reactions.

In the present work we studied the properties and role of surface nitrite, nitrate, and nitro-organic compounds in the selective reduction of nitrogen oxides with hydrocarbons on oxide catalysts, including commercial catalysts NTK-10-1, STK, and Ni–Cr oxide, as well as catalysts on the basis of ZrO_2 (massive ZrO_2, columnar clay with ZrO_2 stacks (ZrO_2–CC), and Pt- and Cu-modified columnar clay (Pt,Cu/ZrO_2–CC).

EXPERIMENTAL

Characteristics of the catalysts used (NTK-10-1, STK, and Ni–Cr oxide) are described in [43–45]. The mechanical mixture was prepared by mixing (without grounding and pressing) individual compounds (fraction 1–2 mm) taken in quantities of 0.6 g each. The catalysts on the basis of ZrO_2 were prepared and characterized as described in [46–48].

The transmission and diffuse reflectance IR spectra were measured on a Perkin–Elmer Spectrum RX-1 FTIR System spectrometer, resolution 4 cm^{-1}, scan time 4.2 s. Computer processing of the spectra was performed using Perkin–Elmer Spectrum software. The IR spectra in two modes: transmission, with a higher sensitivity in the low-frequency spectral range (<1400 cm^{-1}), and diffuse reflectance (DR) in the high-frequency IR range (> 1800 cm^{-1}) to obtain the most complete spectral pattern. The IR spectra at an elevated temperature were measured in an IR reactor cell [49]. The sample for measuring the DR spectra was 1000–1200 mg and for measuring the transmission spectra, 40–60 mg. The intensity of absorption bands in the DR spectra was measured in Kubelka–Munk units and in the transmission spectra, in optical density units. The composition of desorbed products was determined in vacuum experiments with mass spectra analysis on an MKh 7303 instrument.

The spectral kinetic measurements involved simultaneous measurement of catalyst activity and spectrum of surface compounds [50]. The aim of such measurements was to reveal the role of surface complexes in the process in focus. Spectral kinetic measurements in the steady-state and nonsteady-state modes make it possible to determine the rate of transformation of a surface complex and to compare it with the reaction rate.

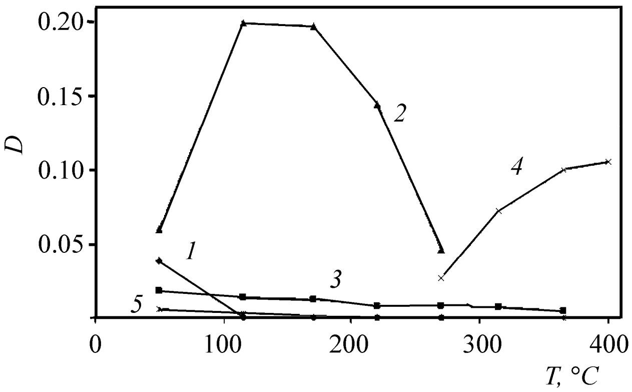

Fig. 1. Dependences of the intensity of the absorption bands on the temperature of the selective reduction of nitrogen oxide with propane on the NTK catalyst. Gas mixture ($0.1\%NO + 0.5\%C_3H_8 + 2.5\%O_2$)/$N_2$. Absorption frequency, cm^{-1}: (*1*) 215, (*2*) 1280, (*3*) 2970; (*4*) 1500, and (*5*) 1630.

The concentrations of reagents in the starting mixtures were varied in the following ranges: 0–0.22% NO, 0–0.67% C_aH_b, and 0–3.5% O_2; the reducer was propane or propylene; carrier gas N_2, the flow rate of the reaction mixture was 150 ml min^{-1} (9000 h^{-1}). All gases were purified by conventional procedures on anhydron and ascarite. Gas analysis before and after the reactor cell was performed on a Beckman-951A NO/NO_x chemiluminescent analyzer and Beckman-590 HC/CO analyzer, or chromatographically with a thermal conductivity detector (adsorbent Porapak Q).

RESULTS AND DISCUSSION

Reactivity of Surface Complexes

NTK catalyst. Spectral measurements *in situ* [43, 44] revealed on the surface of the NTK catalyst under the reaction conditions adsorbed propane complexes (2970 cm^{-1}), bridging nitrite (1215 cm^{-1}), and bridging nitrate (1610, 1280, 1020 cm^{-1}). Figure 1 shows the temperature dependences of the concentration of surface complexes (the concentration of nitrate complexes was assessed by the band at 1280 cm^{-1}).

Below we present data on the reactivity of surface nitrite and nitrate complexes toward propane. Nonsteady-state experiments for assessing the transformation constants of surface complexes were performed in the following way. Nitrite or nitrate adsorbed complexes were formed on catalyst surface,

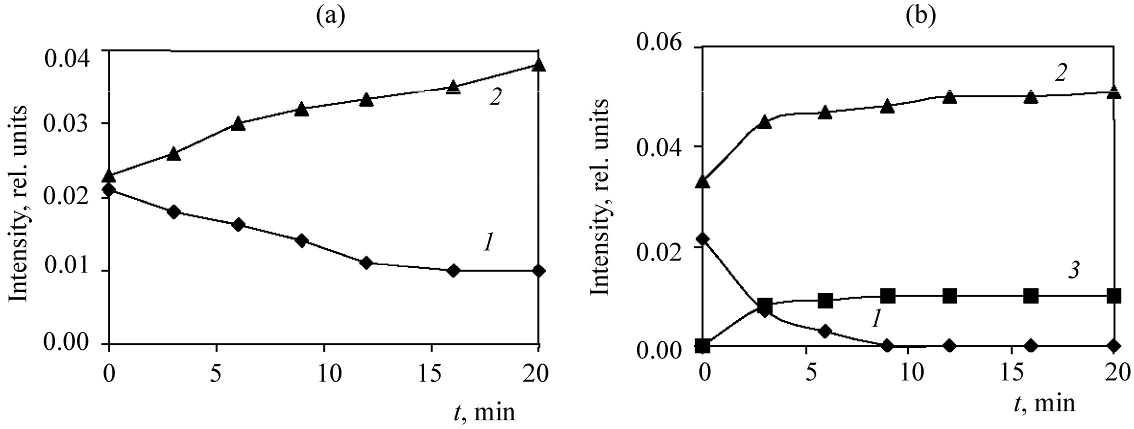

Fig. 2. Dynamics of the absorption intensity of surface (*1*) nitrite and (*2*) nitrate complexes, and (*3*) propane. 115°C. Absorption frequency, cm^{-1}: (*1*) 1215, (*2*) 1280, and (*3*) 2970. Reactant gas: (a) N_2 and (b) C_3H_8/O_2.

after which the IR reactor cell was closed, and the input tubes were purged with the reaction mixture. After a constant gas-phase composition had established in the input tubes, the reaction mixture was fed to the reactor.

From the time dependences of the intensity of the absorption bands of adsorbed complexes, the apparent rate constants of NO_3^- and NO_2^- consumption in a flow of N_2, $0.5\%C_3H_8/N_2$, and $0.5\%C_3H_8 + 2{,}5\%O_2/N_2$ were estimated. Therewith, the time dependences of the intensity of the absorption bands were approximated with a first-order equation in NO_3^- and NO_2^- concentrations, the degree of approximation $R^2 \geq 0.9$.

Figures 2a and 2b show the results of the experiment at 115°C. As nitrogen is fed into the cell (Fig. 2a), the quantity of surface nitrate complexes increases (1280 cm^{-1}) and the quantity of nitrite complexes decreases (1215 cm^{-1}). With C_3H_8/N_2 and $(C_3H_8+O_2)/N_2$, a band at 2970 cm^{-1} appears, and its intensity stabilizes fairly fast (Fig. 2b). Like with nitrogen, the intensity of the band at 1280 cm^{-1} increases with time and that of the band at 1215 cm^{-1} decreases. However, unlike what is observed with nitrogen, the band at 1280 cm^{-1} grows slower, and the band at 1215 cm^{-1} attenuates much faster. The apparent rate constants of the transformation of the nitrate complex on its reaction with a propane–oxygen mixture were estimated at 0.02, 0.08, and 1.1 min^{-1} at 220, 270, and 315°C, respectively.

Surface nitrite complexes, too, were found to be fairly reactive (Table 1). In the presence of propane, the absorption band of the nitrate complex does not grow, and the rate of consumption of the nitrite complex and the rate of nitrate formation at 100°C are close to each other.

The concentration of nitrates on catalyst surface under the conditions of NO_x NS–SCR was determined using the proportionality coefficient A_0 (IR transmission), relating $[NO_3^-]$ to the integral intensity A_{1280} of the nitrate absorption band at 1280 cm^{-1}.

$$[NO_3^-] = A_{1280}/A_0.$$

By combining IR spectroscopy in situ and temperature-programmed desorption (TPD) of NO_x [52] we obtained the coefficient $A_0 = 3.36\times10^{-18}$ cm^{-1}/molecule, and the extinction coefficient by the height of the absorption band was found to be equal to 4.8×10^{-20} cm^2/molecule. The transformation rate constants

Table 1. Transformation characteristics of nitrite and nitrate complexes

T, °C	k_{cons} of nitrite complexes, min^{-1}		Absorption intensity of nitrite complexes under reaction conditions $(0.1\%NO+0.5\%C_3H_8+2.5\%O_2)N_2$	k_{form} of nitrate complexes, min^{-1}
	in N_2	in C_3H_8/N_2		in N_2
115	0.05	0.18	lacking	0.07
100	0.04	–	lacking	0.05
70	0.037	0.045	0.07	0.17

of nitrate complexes, determined in nonsteady-state spectral kinetic experiments, and the quantities of nitrate complexes, determined in steady-state conditions, allowed us to estimate the transformation rate of nitrate complexes and compare it with the rate of the NO_x NS–SCR reaction.

The transformation rate of nitrates for a given sample weight was calculated by the formula $W = kN$, where k is the rate constant and N is the quantity of nitrate complexes for the given sample weight. The reaction rates at different temperatures are compared in Table 2.

The transformation rate of the nitrate complex and the reaction rate at relatively low temperatures are close to each other. The closeness of the rates [51] suggests that the nitrate complex is an intermediate species in NO_x SCR. The transformation rate of the nitrate complex at 315°C is much higher than the reaction rate. Note that the reaction rate decreases as the temperature is increased from 270 to 315°C. The fact that the transformation rate of the nitrate complex is higher than the reaction rate can be explained in terms of the concept that the further reaction step involves formation and consumption of a nitro-organic compound. The intermediacy of these stages was discussed [19–40]. Studies on the transformation pathways of surface nitro-organic compounds showed that in the presence of oxygen these compounds can not only transform into NO_x SCR products, but also undergo further oxidation to form carbon oxides and nitrogen. It is the latter process that occurs in our case. The nitrate complex reacts with an activated propane fragment to give a nitro-organic complex.

The resulting data allow us to suggest the following scheme of the process on the catalyst in focus.

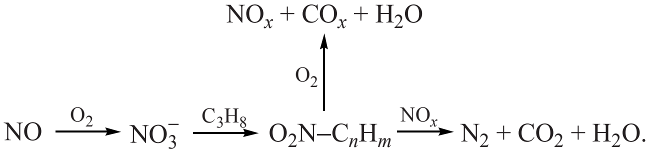

$$\begin{tikzcd} & & NO_x + CO_x + H_2O & \\ NO \arrow[r, "O_2"] & NO_3^- \arrow[r, "C_3H_8"] & O_2N\text{–}C_nH_m \arrow[u, "O_2"] \arrow[r, "NO_x"] & N_2 + CO_2 + H_2O. \end{tikzcd}$$

Note that this scheme is valid at temperatures above 150°C, when the concentration of nitrite complexes on the surface is negligibly low. It should also borne in mind that nitrite complexes are highly reactive at lower temperatures (Figs. 2a and 2b).

The transformation rate of nitrites is close to the reaction rate at 70°C, and at 100°C the steady-state concentration of the nitrite complex is low, and its absorption is obscured by the absorption of the nitrate complex. The transformation rate of the nitrite complex (1215 cm^{-1}) W at 70°C is 1.1×10^{18} complexes/min, and the reaction rate at the same temperature is 1×10^{18} molecules/min. In view of the equality of these two values it is safe to state that the surface nitrite complex at low temperature is an intermediate species in the NO_x SCR reaction. The high reactivity of nitrite complexes can be used for creation of low-temperature catalysts for selective reduction of NO_x with hydrocarbons in the presence of excess oxygen.

STK catalyst. Spectral studies in situ [53] revealed on the surface of the STK catakyst under the reaction conditions a monodentate (1610, 1225, 1030 cm^{-1}) and a bridging (1540, 1260, 1040 cm^{-1}) nitrates, as well as a monodentate nitrite (1410, 1290 cm^{-1}). Further the concentrations of these complexes were estimated from the intensities of the absorption bands at 1610, 1540, and 1290 cm^{-1}. Absorption bands of the acetate complex (1540, 1430, 1250 cm^{-1}) were observed, which could be distinguished from those of the bridging nitrate by varying the temperature and composition of the reaction medium.

The above-described procedure was used to measure the apparent rate constants of consumption of nitrite–nitrate and acetate complexes in the NO_x SCR reaction (Table 3). The resulting data were used to compare the transformation rates of the surface complexes with the reaction rate [51].

The extinction coefficients for estimating the concentration of nitrites on catalyst surface under the

Table 2. Transformation rates of surface nitrate complexes and reaction rates of nitrogen oxides with propane

T, °C	K, min^{-1}	D	$\Delta l_{1/2}$, cm^{-1}	$N_{st,molecule}\times10^{-18}$	$W_{calc}\times10^{-17}$ molecules/min	$W_{exp}\times10^{-17}$ molecules/min
220	0.02	0.095	70	35	7.0	6.8
270	0.08	0.032	50	8.4	6.7	4.1
315	1.10	0.019	20	1.99	22	2.8

Table 3. Comparison of the transformation rates of surface complexes with the rate of selective reduction of NO_x

Surface complex	T, °C, reactant gas	k_{app}, min^{-1}	D_{st}	$\varepsilon \times 10^{19}$, cm^2/molecules	$W_{calc} \times 10^{-17}$ molecules/min at 70 °C	$W_{exp}{}^{a} \times 10^{-17}$ molecules/min at 70 °C
Nitrite (1290 cm^{-1})	70°C $(0.5\%C_3H_6 + 2.5\%O_2)/N_2$	0.005	0	1.20	0	
Bridging nitrate (1610 cm^{-1})	70°C $(0.5\%C_3H_6 + 2.5\%O_2)/N_2$	0.012	0.004	0.25	0.42	4.5
Bidentate nitrate (1540 cm^{-1})	70°C $(0.5\%C_3H_6 + 2.5\%O_2)/N_2$	0.008	0.035	0.20	3.50	
Acetate (1540 cm^{-1}) (1430 cm^{-1})	220°C $(0.1\%NO + 2.5\%O_2)/N_2$	0.036 0.033	0.024 0.032	7.00	0.27	1.5
Acetate (1540 cm^{-1}) (1430 cm^{-1})	275°C $(0.1\%NO + 2.5\%O_2)/N_2$	0.080 0.075	0.018 0.022	7.00	0.45	3.6

[a] Reactant gas: $(0.1\%NO + 0.5\%C_3H_6 + 2.5\%O_2)/N_2$.

NO_x NS–SCR reaction conditions, found by combining IR spectroscopy and NO_x TPD data, were as follows, cm^2/molecule: $\varepsilon_{1290} = 1.2\times10^{-19}$, $\varepsilon_{1610} = 0.25\times10^{-19}$, and $\varepsilon_{1540} = 0.2\times10^{-19}$. The extinction coefficients for vibrations of the acetate complex were taken from [54], cm^2/molecule: $\varepsilon_{1430} = 3.3\times10^{-19}$, $\varepsilon_{1540} = 7.0\times10^{-19}$.

Using these values and the optical densities of the absorption bands of nitrite, nitrate, and acetate complexes under the reaction conditions, we estimated the transformation rate of nitrate complexes and compared it with the rate the NO_x NS–SCR reaction (Table 3). From the rate constants we could tentatively estimate the activation energy of the transformation of nitrite to nitrate structures and the activation energies of their desorption at 60–80 kJ mol^{-1}.

According to published data (for example, cf. [19, 55]), surface nitrite–nitrate complexes are intermediates in the reduction of nitrogen oxides with hydrocarbons, and they react with an activated hydrocarbon to form a nitro-organic complex that further transforms into reaction products. This conclusion is consistent with the results of our mechanistic study of the reactions on an NTK-10-1 Cu–Zn–Al oxide catalyst and on the STK catalyst. Actually, as seen from Table 3, the total transformation rate of nitrite–nitrate structures on at 70°C is close the rate of NO_x transformation. This result implies that these structures are intermediate species in the NO_x SCR reaction with propane in the presence of excess oxygen.

Shimizu et al. [13, 14, 18] have studied the selective catalytic reduction of NO_x with propylene on Al_2O_3 and Cu/Al_2O_3 to find that the rate of formation of reaction products is determined by the reaction between acetate and nitrate complexes. In our case (Table 3), comparison of the transformation rate of the acetate complex with the reaction rate shows that the reaction of acetate with adsorbed NO_x is only one of reaction pathways, and, therewith, the contribution of this pathway decreases with increasing temperature.

The presented data together allow us to suggest the following mechanism of reduction of nitrogen oxides with propane on the STK catalyst. At temperatures below 250°C, the reduction rate is determined by the reaction of surface nitrite–nitrate complexes with an activated hydrocarbon and further according to the mechanism described in [19, 55]. As the temperature increases, the quantity of nitrite–nitrate complexes fast decreases, and the reaction rate decreases until NO starts to decompose on the reduced surface. Nitrogen atoms recombine to form molecular nitrogen in the gas phase. This fact is confirmed by the results of TPD with mass spectral analysis of desorption products, the main of which is molecular nitrogen. Oxygen atoms react with the hydrocarbon to form CO_2.

To conclude, we would like to mention that the differences on the mechanisms of the NO_x NS–SCR reactions on the STK and NTK-10-1 catalysts is due to the absence of high-temperature NO adsorption on STK and a higher reducibility of the latter in the reaction mixture. Another feature of the STK catalyst is its ability to form soft propane oxidation products. Probably, these circumstances explain the synergistic effect of mechanical mixtures of the STK and NTK-10-1 catalysts [52, 53].

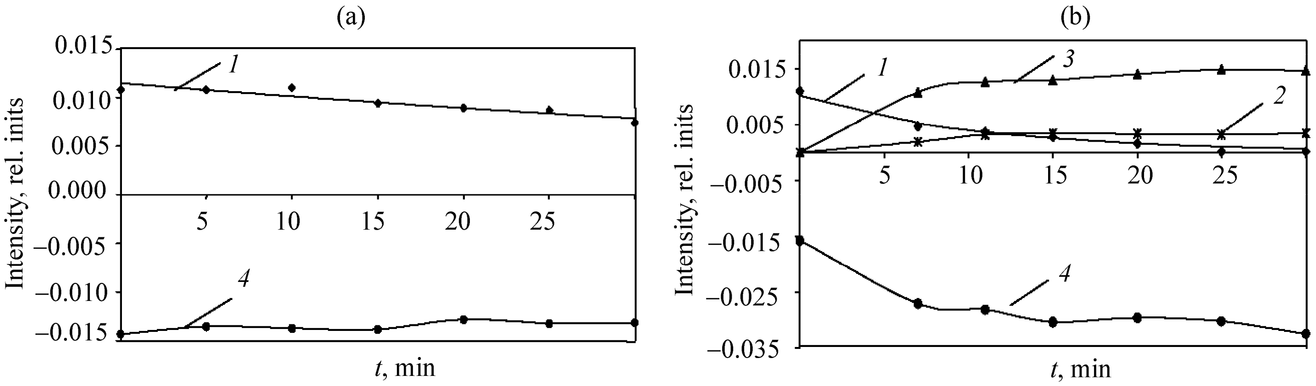

Fig. 3. Dynamics of the absorption intensity of surface nitrite–nitrate compounds at 150°C on the nickel–chromium catalyst. Absorption frequency, cm^{-1}: (*1*) 1290, (*2*) 1425, (*3*) 1550, and (*4*) 1000. Reactant gas: (a) N_2 and (b) $(0.5\%C_3H_8+2.5\%O_2)/N_2$.

Nickel–Chromium Catalyst. Figure 3 shows the results of a typical experiment on the reaction of nitrate complexes with N_2 and $(0.5C_3H_8 + 2.5O_2)/N_2$ flows at 150°C on a nickel–chromium catalyst. The intensity of the absorption bands of nitrate structures under $(C_3H_8 + O_2)/N_2$ (Fig. 3b) decreases much stronger than under N_2 (Fig. 3a), implying that nitrate complexes react with propane. Note that, as nitrate complexes are consumed, the absorption bands of acetate complexes grow (Fig. 3b, curves *2* and *3*).

These dependences were approximated by a first-order equation in NO_3^- concentration, the degree of approximation R^2 was no less than 0.9. The resulting apparent rate constants (k_{app}) of consumption of nitrate complexes on their reaction with $(0.5C_3H_8 + 2.5O_2)/N_2$, estimated by the band at 1280 cm^{-1}, are shown in Table 4.

Figure 4 shows the dynamics of the intensity of the absorption bands of acetate complexes (1550, 1425, and 1350 cm^{-1}) on their reaction with N_2 (Fig. 4a) and $(0.1NO + 2.5O_2)/N_2$ (Fig. 4b) flows at 300°C. The kinetic curves tend to straight lines in the coordinates of a first-order. Thus we determined the apparent consumption rate constants by all the three absorption bands of acetate complexes (1550, 1425, and 1350 cm^{-1}). Table 5 lists k_{app} averaged over those determined by the three bands.

To assess the role of surface complexes, we compared their transformation rates with the reaction rate. The extinction coefficients for nitrate complexes were determined from spectral and thermodesorption experimental data [52, 53]. Note that these coefficients for nitrate structures are fairly close to those obtained earlier for the Fe–Cr oxide catalyst STK. The extinction coefficients of the absorption bands at 1425 and 1550 cm^{-1} of the acetate complex were taken from [54], cm^2/molecule: $\varepsilon_{1425} = 3.3\times10^{-19}$ and $\varepsilon_{1550} = 7.0\times10^{-19}$.

The results of comparison of the transformation rate of surface nitrate complexes with the rate of the NO_x

Table 4. Comparison of the transformation rate of surface nitrate complexes with the rate of the NO_x NS-SCR reaction[a]

T, °C	k_{app}, min^{-1}		D_{st}	$\varepsilon\times10^{19}$, cm^2/molecules	$W_{calc}\times10^{-17}$ molecules/min	$W_{exp}\times10^{-17}$ molecules/min
	N_2	$C_3H_8 + O_2/N_2$				
70	0.0033	0.0032	0.0137	0.3±0.1	0.015	0
100	0.0066	0.0100	0.0146		0.049	
125	0.0090	0.0190	0.0135		0.086	
150	0.0084	0.0923	0.0116		0.360	
175	0.0127	0.2260	0.0076		0.570	
200	0.0381	0.5596	0.0035		0.640	

[a] Reactant gas $(0.1\%NO + 0.5\%C_3H_8 + 2.5\%O_2)/N_2$. Sample weight 25 mg.

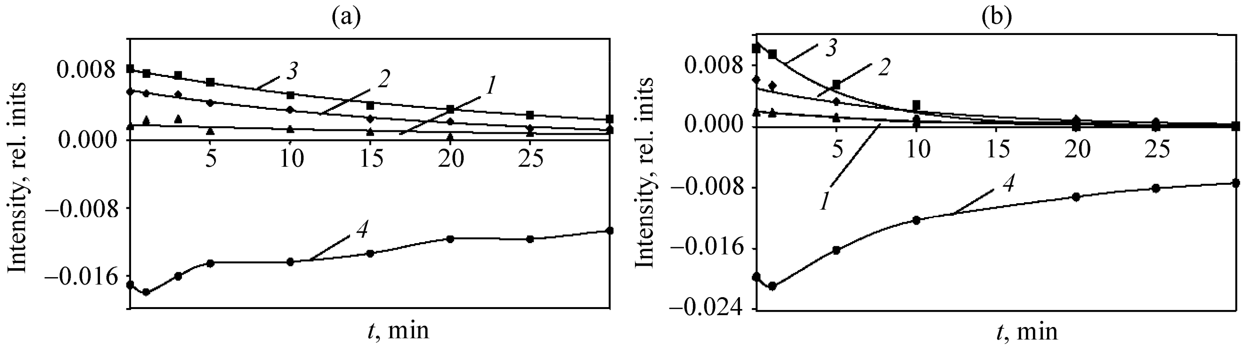

Fig. 4. Dynamics of the absorption intensity of surface acetate complexes at 300°C on the nickel–chromium catalyst. Absorption frequency, cm^{-1}: (*1*) 1350; (*2*) 1425; (*3*) 1550; and (*4*) 1000. Reactant gas: (a) N_2 and (b) (0.1% NO + 2.5%O_2)/N_2.

HC–SCR reaction are listed in Table 4. At 100–200°C, surface nitrate structures fairly fast react with propane. At the same time, no conversion of nitrogen oxides in this temperature range is observed. To provide evidence for this finding, we also performed conversion measurements using a sample whose weight was 50 times that specified in Table 4 (1250 mg). No conversion of nitrogen oxides was observed. At the same time, estimates based on the transformation rates of nitrate complexes show that the conversion of nitrogen oxides at the sample weight 1250 mg at 100°C should be ~5% and at 200°C, ~60%.

The above data together imply that nitrate complexes are involved in a process that does not form reaction products. For example, Valverde et al. [56] and Chi and Chuang [57] considered expulsion of nitrates stabilized on Cu^{2+} ions incorporated in columnar clay, as they react with $C_3H_6 + O_2$ flow. In our case, such process is accompanied by formation and accumulation of acetate complexes, probably, with NO_x evolution. In other words, surface nitrate complexes function to activate propane but take no part in forming reaction products. The presence of oxygen in a mixture with propane has almost no effect on this process.

Indirect evidence showing that the propane activation process involves no formation of reaction products is provided by the absence of any complexes in further nitrate transformations. Note that the reaction of nitrates and acetate strictures on ZrO_2-based catalysts forms a nitro-organic complex (see below).

The reaction between acetate and nitrate complexes was found to be the rate-limiting stage of the selective catalytic reduction of NO_x with propylene on Al_2O_3 and Cu/Al_2O_3 [13, 14, 18]. In our case, acetate complexes in their reaction with the $(0.1NO + 2.5O_2)/N_2$ mixture are consumed at an appreciable rate (Table 5). The following apparent rate constants of consumption of acetate complexes in their reactions with N_2, $2.5O_2/N_2$, $0.1NO/N_2$, and $(0.1NO+2.5O_2)/N_2$ at 250°C:

$$k(N_2) = 0.008,\ k(2.5\%O_2/N_2) = 0.0363,$$
$$k(0.1\%NO/N_2) = 0.0733,$$
$$k(0.1\%NO + 2.5\%O_2/N_2) = 0.110\ \text{min}^{-1}.$$

As seen, the consumption of acetate complexes is mostly contributed by their reaction with nitrogen

Table 5. Comparison of the transformation rate of surface acetate complexes with the rate of the NO_x NS–SCR reaction[a]

T, °C	k_{app}, min^{-1}		D_{st}	$\varepsilon\times10^{19}$, cm^2/molecules	$W_{calc}\times10^{-17}$ molecules/min	$W_{exp}\times10^{-17}$ molecules/min
	N_2	$(0.1NO + 2.5O_2)/N_2$				
225	~0	0.017	0.0057	7.0	0.0320	0.128
250	0.0080	0.110	0.0066		0.0194	0.256
275	0.0170	0.160	0.0075		0.0410	0.297
300	0.0557	0.310	0.0069		0.0690	0.400

[a] Reactant gas $(0.1\%NO + 0.5\%C_3H_8 + 2.5\%O_2)/N_2$. Sample weight 25 mg.

oxide and oxygen. It can be suggested that this surface reaction completes the deep propane oxidation process, whereas the reaction of acetate complexes with nitrogen oxide is involved in the NO_x reduction process.

Analysis of the data in Table 5 shows that NO_x NS–SCR at temperatures above 200°C occurs much faster that the reaction of the acetate complex with the $(0.1NO + 2.5O_2)/N_2$ mixture.

Let us consider the possible reaction pathways at elevated temperatures. The nickel–chromium catalyst is partially reduced at elevated temperatures in the presence of the reaction mixture. On the reduced surface (according to the results of NO TPD with mass spectral analysis), the major fraction among the NO desorption products is molecular nitrogen. This fact implies NO decomposition. Nitrogen atoms recombine, and oxygen atoms reoxidize the surface to form on it oxygen-containing centers. Activated hydrocarbon species can react with these centers, thus regenerating the reduced surface.

The reduction of nitrogen oxides with propane on the Ni–Cr catalyst at temperatures of up to 200°C forms surface acetate complexes, and the reaction stops at this stage. As the temperature is raised further, acetate complexes are involved in reaction, and the NO decomposition reaction begins on the reduced surface. As a result, nitrogen atoms recombine to form molecular nitrogen, and oxygen atoms react with the activated hydrocarbon (probably, in a radical form) to form water and CO_2, thereby regenezating the active surface center.

Reduction of Nitrogen Oxides with Propylene on ZrO_2-Based Catalysts

The spectra measured during reaction of the reaction mixture with the surface of columnar clay (Pt, Cu/ZrO_2–CC) in the range 50–200°C contain overlapping absorption bands of the isopropoxide propylene complex, coordinated acetone, and nitrates. Bands at 1386, 1435, 1575, 2993, 2942, 2920, and 2885 cm^{-1} are also observed, which, in agreement with published data [30–36], can be assigned to symmetric, stretching and deformation C–H vibrations in the nitro-organic surface complex. Further evidence for this assignment is provided by the fact that, in the absence of NO or C_3H_6 in the gas phase these absorption bands are not observed. Our nonsteady-state spectral experiments showed that the above bands relate to vibrations in a single surface complex [47].

The structure of the nitro-organic complex was established by studying adsorption of various nitro-organic compounds (nitromethane, nitroethane, and 1-nitropropane) at 150°C [46–48]. These data, as well as data reported in [58, 59], make us to suggest the structure of the nitro-organic complex under the reaction conditions is lose to the structure of adsorbed dinitropropane. The addition of two NO_2 groups to propylene during selective catalytic reduction of NO_x on zeolite catalysts has been considered in [60, 61].

In the range 250–400°C, the intensity of all absorption bands decreases, but the band of the nitro-organic compounds also changes its position: The antisymmatric vibration band of the nitro group shifts to lower frequencies, and the half-width of the symmetric vibration band increases to form a band with ill-resolved maxima at 1392 and 1382 cm^{-1}. Figure 5 (spectra *1* and *4*) shows for comparison the spectra of nitromethane adsorbed at 150 and 300°C. As seen, as the reaction temperature is increased, the intensity and splitting of the bands at 1402 and 1379 cm^{-1} decrease, and at 300°C the spectra show an ill-resolved doublet with maxima at 1395 and 1387 cm^{-1}. These results can be explained under the assumption that, at increased reaction temperature, when the isopropoxide complex is no longer present on the surface, the acetate and nitrate complexes form a nitro-organic complex that is structurally similar to adsorbed nitromethane, like in the case of massive ZrO_2.

On the surface of Pt,Cu/ZrO_2–CC, unlike ZrO_2–CC, two forms of propylene activation are possible: low-temperature (isopropoxide) and high-temperature (acetate). Apparently, this fact explains why there are two different nitro-organic complexes in different temperature ranges: dinitropropane at low temperatures and nitromethane at high temperatures.

To find out the role of nitrate and hydrocarbon complexes in the formation of nitro-organic intermediates, we accomplished a series of nonsteady-state experiments. Surface nitrate complexes were formed by exposure of sample surface to the $(0.2\%NO + 2.5\%O_2)/N_2$ flow. The IR cell with the sample was then purged with nitrogen, after which the $(0.2\%C_3H_6 + 2.5\%O_2)/N_2$ mixture was fed, and absorption intensity of surface compounds was monitored.

Quantitative characteristics of the transformation of nitrate complexes under NO_x SCR conditions on Pt,Cu/ZrO_2–CC and ZrO_2–CC are presented in

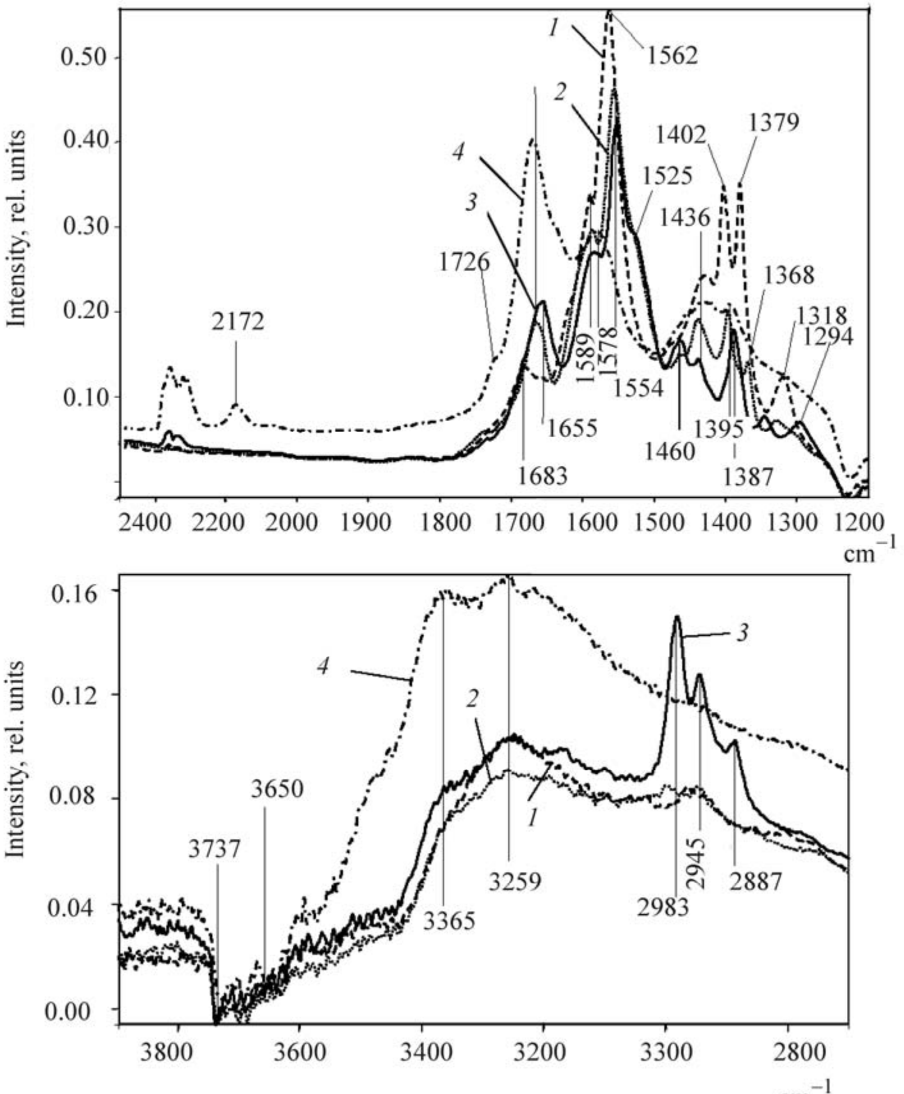

Fig. 5. IR spectra of surface compounds, measured during reaction of nitro compounds with the Pt, Cu/ZrO_2–CC surface. 150°C. Compound: (*1*) nitromethane, (*2*) nitroethane, and (*3*) nitropropane. (*4*) Adsorption of nitromethane at 300°C.

Table 6. The procedure for the determination of reaction rate constants and concentrations of surface nitrate complexes have been described in detail in [49, 51].

There are two conclusion following from the data in Table 6:

– the transformation rate of nitrate complexes is close to the NO_x SCR rate, implying that nitrates play the role of intermediates in this reaction;

– the reactivity of nitrate complexes increases considerably in going from massive ZrO_2 to ZrO_2–CC, and further to the modified columnar clay Pt, Cu/ZrO_2–CC.

The results of nonsteady-state measurements show that the major source of the nitro-organic compound in this case is bridging nitrate. Surface hydrocarbon complexes were formed by exposure of the sample surface to ($0.2\%C_3H_6 + 2.5\%O_2$)/N_2 at various temperatures. Then the cell with the sample was purged with an inert gas and the ($0.2\%NO + 2.5\%O_2$)/N_2 mixture, and, therewith, absorption intensity of surface compounds was monitored.

At 100°C no other species than isopropoxide complexes are formed on the surface, and they are not removed when the catalyst is exposed to an inert gas. After the ($0.2\%NO + 2.5\%O_2$)/N_2 mixture has been fed, isopropoxide complexes start to be rapidly consumed

Table 6. Characteristics of the transformation of surface nitrate complexes

Catalyst	T, °C	Apparent transformation rate constant of nitrate complexes k_1, min^{-1}	Transformation rate of nitrate complexes, $W\times10^{-18}$, molecule/min	Reaction rate, $W\times10^{-18}$, molecule/min	Reference
ZrO_2	400	0.038	5.0	5.6	[46]
ZrO_2–CГ	250	0.035	2.0	1.8	[47]
Pt, Cu/ZrO_2–CГ	150	0.070	2.7	3.0	[48]

Table 7. Characteristics of the transformation of surface nitro-organic complexes

Catalyst	T, °C	Apparent transformation rate constant of nitro-organic complexes k, min^{-1}
ZrO_2	350	0.032
ZrO_2–CГ	250	0.040
Pt,Cu/ZrO_2–CГ	150	0.070

(Fig. 6, curve *3*); simultaneously the concentrations of acetone and nitro-organic compounds increase (Fig. 6, curves *1* and *2*). This implies that both the nitro-organic compounds and acetone are formed from the isopropoxide complex.

Figure 7 shows the IR spectra measured in the course of the reactions of acetate complexes with N_2 (spectrum *1*) and (0.2%NO+2.5%O_2)/N_2 (spectrum *2*) at 300°C. In the course of the reaction of acetates with (0.2%NO + 2.5%O_2)/N_2, the spectra show a weak broad absorption band at 1390–1380 cm^{-1}, analogous ti that of nitromethane adsorbed at 300°C (Fig. 5). The same band, while more intense, was observed in the spectra obtained during the reaction of the (0.2%NO + 0.2%C_3H_6 + 2.5%O_2)/N_2 mixture with sample surface. Consequently, at fairly high temperatures acetate complexes can be a source for a nitro-organic complex structurally similar to adsorbed nitromethane.

In the same way we studied the reactivity of a nitro-organic complex formed by the reaction of (0.2%NO + 0.2%C_3H_6+2.5%O_2)/N_2 with catalyst surface. Quantitative characteristics of nitro-organic complexes under conditions of the NO_x SCR reactions on Pt,Cu/ZrO_2–CC, ZrO_2, and ZrO_2–CC are presented in Table 7.

As seen, k increases in going from massive ZrO_2 to ZrO_2–CC, and further to Pt, Cu/ZrO_2–CC. Furthermore, the rate constants of consumption of nitro-organic and nitrate complexes for all the catalysts studied are close to each other (Tables 6 and 7), and these complexes can be real intermediate in selective catalytic reduction of NO_x with propylene.

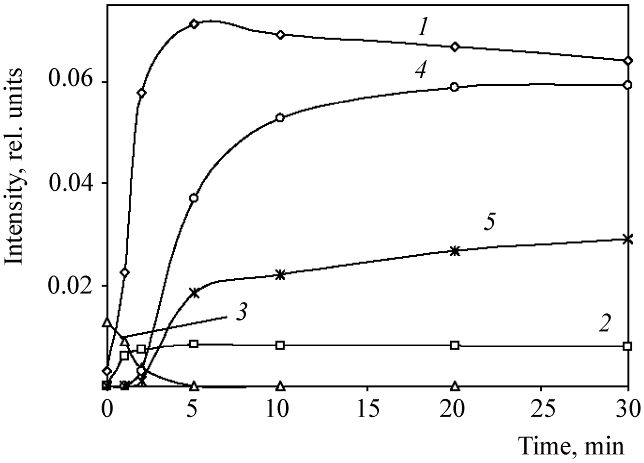

Fig. 6. Dynamics of the absorption intensity of surface complexes on modified columnar clay, 100°C. Reactant gas (0.2%NO + 2.5%O_2)/N_2. Complex: (*1*) acetone, (*2*) nitro-organic, (*3*) isopropoxide, and (*4*) bridging, and (*5*) bidentate nitrate.

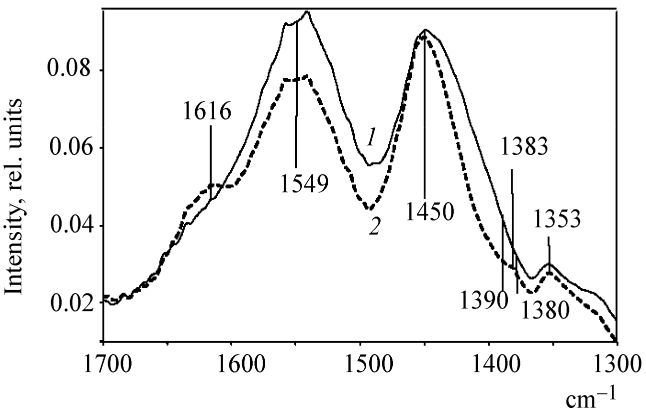

Fig. 7. IR spectra obtained on exposure of the acetate complex preformed on the Pt,Cu/ZrO_2–CC surface at 300°C to (*1*) N_2 and (*2*) (0.2%NO + 2.5%O_2)/N_2.

Experiments involving exposure of surface nitro-organic complexes to 2.5%O_2/N_2 and 0.2%NO/N_2 flows. The concentration of nitro-organic complexes under both 2.5%O_2/N_2 and 0.2%NO/N_2 decreased at the same rate as with N_2. This finding implies that nitro-organic compounds are consumed due to the presence of NO_2 complexes under the reaction conditions. Since the equilibrium NO_2 concentration at elevated temperatures is low, the formation of such complexes on the surface is associated with the decomposition of nitrates.

The spectral kinetic study of the process on ZrO_2-containing catalysts showed that the difference in the forms of catalyst activation results in that structurally different nitro-organic complexes are formed. On massive ZrO_2, acetate and nitrate complexes form a structure similar to adsorbed nitromethane. A monodentate nitrate is the most active in this process. At relatively low temperatures, isopropoxide and nitrate on modified and unmodified ZrO_2 columns form a structure close to adsorbed dinitropropane.

Thus, the results of our study show that the initial stages of selective reduction of nitrogen oxides with hydrocarbons involve formation of surface nitrite–nitrate structures and hydrocarbon activation. Nitrates react with the activated hydrocarbon to form nitro-organic compounds whose structure is determined by the form of hydrocarbon activation. The nitro-organic compound decomposes on reaction with $NO_x + O_2$ to give molecular nitrogen.

REFERENCES

1. Iwamoto, M., Yahiro, H., Yu-u, Y., Shundo, S., and Mizuno, N., *Shokubai*, 1990, vol. 32, p. 430.
2. Held, W., Kogin, A., Richter, T., and Puppe, L., in: *Catalytic NO$_x$ Reduction in Net Oxidizing Exhaust Gas*, SAE Technical Paper Series 900496, 1990, p. 13.
3. Matyshak, V.A., Il'ichev, A.N., Ukharsky, A.A., and Korchak, V.N., *J. Catal*., 1997, vol. 171, p. 245.
4. Gopalakrishnan, R., Stafford, P.R., Davidson, J.E., et al., *Appl. Catal. B*, 1993, vol. 2, p.165.
5. Kharas, K.C.C., *Ibid.*, 1993, vol. 2, p. 207.
6. Shapiro, E.S., Joyner, W.R., Grunert, W., et al., *Stud. Surf. Sci. Cat*., 1994, vol. 84, p. 1483.
7. Larsen, S.C., Aylor, A., Bell, A.T., and Reimer, J.A., *J. Phys. Chem*., 1994, vol. 98, p. 11533.
8. Genti, G. and Perathoner, S., *Appl. Catal. A*, 1995, vol. 132, p. 179.
9. Ivamoto, M., *Catal. Today*, 1996, vol. 29, p. 29.
10. Amiridis, M.D., Zhang, T., and Farrauto, R.J., *Appl. Catal. B*, 1996, vol. 10, p. 203.
11. Sadykov, V.A., Beloshapkin, S.A., Paukshtis, E.A., et al., *Polish J. Environ. Stud*., 1997, vol. 6, Suppl., p. 21.
12. Sirilumpen, M., Yang, R.T., and Tharapiwattananon, N., *J. Mol. Catal. A: Chem*., 1999, vol. 137, p. 273.
13. Shimizu, K., Kawabata, H., Maeshima, H., Satsuma, A., and Hattori T., *J. Phys. Chem*., 2000, vol. 104, p. 2885.
14. Shimizu, K., Kawabata, H., Satsuma, A., and Hattori, T., *Ibid*., 1999, vol. 103, p. 5240.
15. Chi, Y. and Chuang, S.S.C., *J. Catal*., 2000, vol. 190, p. 75.
16. Satsuma, A., Enjoji, T., Shimizu, K., et al., *J. Chem. Soc*., 1998, vol. 94, p. 301.
17. Petunchi, J.O. and Hall, W.K., *Appl. Catal. B*, 1993, vol. 2, p. 17.
18. Shimizu, K., Shibata, J., Yoshida, H., Satsuma, A., and Hattori, T., *Ibid*., 2001, vol. 30, p. 151.
19. Burch, R., Breen, J.P., and Meunier, F.C., *Ibid*., 2002, vol. 39. p. 283.
20. Gorce, O., Baudin, F., Thomas, C., et al., *Ibid*., 2004, vol. 549, p. 69.
21. Anderson, J.A. and Rochester, C.H., *J. Chem. Soc., Faraday Trans*., 1989, vol. 185, p. 1117.
22. Anderson, J.A. and Rochester, C.H., *Ibid*., 1989, vol. 185, p. 1129.
23. Yeom, Y.H., Wen, B., Sachtler, W.M.H., and Weitz, E., *J. Phys. Chem*. B, 2004, vol. 108, p. 5386.
24. Yeom, Y.H., Li, M., Sachtler, W.M.H., and Weitz, E., *J. Catal*. 2007, vol. 246, p. 413.
25. Li, M., Yeom, Y.H., Weitz, E., and Sachtler, W.M.H., *Ibid*., 2005, vol. 235, p. 201.
26. Sun, Q., Gao, Z.X., Chen, H.Y., and Sachtler, W.M.H., *Ibid*., 2001, vol. 201, p. 89.
27. Haneda, M., Kintaichi, Y., Inaba, M., and Hamada, H., *Catal. Today*, 1998, vol. 42. p. 127.
28. Yokoyama, C. and Misono, M., *Ibid*., 1994, vol. 22, p. 59.
29. Gerlach, T. and Baerns, M., *Chem. Eng. Sci*., 1999, vol. 54, p. 4379.
30. Hadjiivanov, K.I., *Catal. Rev.-Sci. Eng.,* 2000, vol. 42, p. 71.
31. Adelman, B., Beutel, T., Lei, G., and Sachtler, W.M.H., *J. Catal*., 1996, vol. 158, p. 327.
32. Meunier, F.C., Breen, J.P., Zuzaniuk, V., et al., *Ibid*., 1999, vol. 187, p. 493.
33. Tanaka, T., Okuhara, T., and Misono, M., *Appl. Catal*., 1994, vol. 4, L1.
34. Sumiya, S., He, H., Abe, A., et al., *J. Chem. Soc., Faraday Trans*., 1998, vol. 94, p. 2217.
35. Maunula, T., Ahola, J., and Hamada, H., *Appl. Catal. B*, 2000, vol. 26, p. 173.

36. Chi, Y. and Chuang, S.S.C., *J. Catal*., 2000, vol. 190, p. 75.
37. Finocchio, E., Busca, G., Lorenzelli, V., and Willey, R.J*.*, *J. Shem. Soc., Faraday Trans*., 1994, vol. 90, p. 3347.
38. Captain, D.K. and Amiridis, M.D., *J. Catal*., 2000, vol. 194, p. 222.
39. Radtke, F., Koeppel, R. A., and Baiker, A., in: *Environmental Catalysis*, Rome: SCI, 1995.
40. Bamwenda, G.R., Ogata, A., Obuchi, A., et al., *Appl. Catal. B*, 1995, vol. 6, p. 311.
41. Long, R.Q. and Yang, R.T., *J. Phys. Chem. B*, 1999, vol. 103, p. 2232.
42. Ukisu, Y., Sato, S., Muramatsu, G., and Yoshida, K., *Catal. Lett*., 1991, vol. 11, p. 177.
43. Matyshak, V.A., Korchak, V.N., Tret'yakov, V.F., et al., *Kinet. Katal*., 2003, vol. 44, p. 915.
44. Tret'yakov, V.F., Matyshak, V.A., Burdeinaya, T.N., et al., *Ibid*., 2005, vol. 46, p. 550.
45. Tret'yakov, V.F., Zakirova, A G., Matyshak, V.A., et al., *Ibid*., 2006, vol. 47, p. 900.
46. Matyshak, V.A., Chernyshov, K.A., Korchak, V.N., et al., *Ibid*., 2006, vol. 47, p. 770.
47. Matyshak, V.A., Chernyshov, K.A., Korchak, V.N., et al., *Ibid*., 2006, vol. 47, p. 610.
48. Matyshak, V.A., Chernyshov, K.A., Korchak, V.N., et al., *Ibid*., 2007, vol. 48, p. 81.
49. Matyshak, V.A. and Krylov, O.V., *Catal. Today*, 1995, vol. 25, p. 1.
50. Matyshak, V.A., *Kinet. Katal*., 1997, vol. 38, p. 432.
51. Krylov, O.V. and Matyshak, V.A., *Promezhutochnye soedineniya v geterogennom katalize* (Intermediate Compounds in Heterogeneous Catalysis), Moscow: Nauka, 1996.
52. Matyshak, V.A., Korchak, V.N., Tret'yakov, V.F., et al., *Kinet. Katal.,* 2003, vol. 44, p. 921.
53. Tret'yakov, V.F., Burdeinaya, T.N., Zakorchevnaya, Yu.P., et al., *Kinet. Katal*., 2005, vol. 46, p. 559.
54. Matyshak, V.A. and Krylov, O.V., *Ibid*., 2002, vol. 43, p. 422.
55. Sadykov, V.A., Lunin, V.V., Matyshak, V.A., et al., *Ibid*., 2003, vol. 44, p. 412.
56. Valverde, J.L., de Lucas, A., Dorado, F., et al., *J. Mol. Catal. A: Chem*., 2005, vol. 230, p. 23.
57. Chi, Y. and Chuang, S.S.C., *J. Catal*., 2000, vol. 190, p. 75.
58. Paperno, T.Ya. and Perekalin, V.V., *Infrakrasnye spektry nitrosoedinenii* (Infrared Spectra of Nitro Compounds), Leningrad: Len. Gos. Univ., 1974.
59. Noble, P., Borgardt, F.G., and Reed, W.L., *Chem. Rev*., 1964, vol. 64, p. 19.
60. Yokoyama, C. and Misono, M., *J. Catal*., 1994, vol. 150, p. 9.
61. Martens, J.A., Cauvel, A., Francis, A., et al., *Angew. Chem., Int. Ed*., 1998, vol. 37, p. 1901.